의학박사 학위논문

Comparative analysis of the pathophysiological characteristics of *ALK*-rearranged lung adenocarcinoma based on driver oncogene mutations

ALK 유전자 전위 폐선암의 병태생리학적 특성

- 암 유전자 변이에 따른 비교 분석 연구 -

2015년 2월

서울대학교 대학원

의학과 병리학전공

김 효 진

ALK 유전자 전위 폐선암의 병태생리학적 특성

- 암 유전자 변이에 따른 비교 분석 연구 -

지도교수 정 진 행

이 논문을 의학박사 학위논문으로 제출함

2014년 10월

서울대학교 대학원

의학과 병리학 전공

김 효 진

김효진의 의학박사 학위논문을 인준함

2014년 12월

위 원 장 _____ (인)

부위원장 _____ (인)

위 원 _____ (인)

위 원 _____ (인)

위 원 _____ (인)

Comparative analysis of the pathophysiological characteristics of *ALK*-rearranged lung adenocarcinoma based on driver oncogene mutations

by
Hyojin Kim

A thesis submitted to the Department of Medicine in partial fulfillment of the requirements for the Degree of Doctor of Philosophy in Medical Science (Pathology) at Seoul National University College of Medicine

December, 2014

Approved by Thesis Committee:

Professor _____Chairman
Professor _____Vice chairman
Professor _____
Professor _____
Professor _____

Abstract

Comparative analysis of the pathophysiological characteristics of *ALK*-rearranged lung adenocarcinoma based on driver oncogene mutations

Hyojin Kim

Department of medicine, Major in pathology

The Graduate School

Seoul National University

Introduction: Molecular classification of lung cancer correlates well with histomorphological features. However, specific histomorphological features that differentiate anaplastic lymphoma kinase (*ALK*)-rearranged tumors from *ALK*-negative tumors have not been fully evaluated.

Methods: Eighty *ALK*-rearranged and 213 *ALK*-negative (91 *epidermal growth factor receptor*-mutated; 29 *K-ras* mutated; 93 triple-negative) resected lung adenocarcinomas were analyzed for several histomorphological parameters and

histological subtypes.

Results: *ALK*-rearranged tumors were associated with younger age at presentation, frequent nodal metastasis, and higher stage of disease at diagnosis. *ALK*-rearranged tumors were more likely to show a solid predominant pattern than *ALK*-negative tumors (43.8%; 35/80; $p<0.001$). Unlike *ALK*-negative tumors, a lepidic predominant pattern was not observed in *ALK*-rearranged tumors ($p<0.001$). In multivariate analysis, the most significant morphological features that distinguished *ALK*-rearranged tumors from *ALK*-negative tumors were cribriform formation (odds ratio [OR], 3.253; $p=0.028$), presence of mucin-containing cells (OR, 4.899; $p=0.008$), close relationship to adjacent bronchioles (OR, 5.361; $p=0.001$), presence of psammoma bodies (OR, 4.026; $p=0.002$), and a solid predominant pattern (OR, 13.685; $p=0.023$). *ALK*-rearranged tumors exhibited invasive histomorphological features, aggressive behavior and frequent expression of epithelial-mesenchymal transition markers (loss of E-cadherin and expression of vimentin) compared with other genotype ($p=0.015$). Spatial proximity between bronchus and *ALK*-rearranged

tumors and frequent solid histologic subtype with p63 expression may cause diagnostic difficulties to differentiate squamous cell carcinoma in the small biopsy, whereas p40 was rarely expressed in *ALK*-rearranged adenocarcinoma.

Conclusion: *ALK*-rearranged lung adenocarcinoma exhibited distinct clinicopathological and morphological features compared with other genotypes. Knowledge of these features may improve the diagnostic accuracy and lead to a better understanding of the characteristic behavior of *ALK*-rearranged tumors.

* This work is published in PLoS ONE (Kim H, Jang SJ, Chung DH, Yoo SB, Sun P, Jin Y et al. A comprehensive comparative analysis of the histomorphological features of *ALK*-rearranged lung adenocarcinoma based on driver oncogene mutations: frequent expression of epithelial-mesenchymal transition markers than other genotype. PLoS ONE. 2013 Oct; 8(10): e76999.)

Keywords: Lung neoplasms, Adenocarcinoma, Anaplastic lymphoma kinase, Histology, Genotype

Student Number: 2012-30544

Contents

List of Tables

List of Figures

List of Abbreviations and Symbols

ALK	Anaplastic lymphoma kinase
EGFR	Epidermal growth factor receptor
FISH	Fluorescence *in situ* hybridization
NSCLC	Non-small cell lung cancer
IASLC	International Association for the Study of Lung Cancer
ATS	American Thoracic Society
ERS	European Respiratory Society
EMT	Epithelial-mesenchymal transition
CSC	Cancer stem cell
TN	Triple negative
H&E	Hematoxylin and eosin
IMA	Invasive mucinous adenocarcinoma
FFPE	Formalin fixed paraffin embedded

IHC	Immunohistochemistry
PCR	Polymerase chain reaction
MUC	Mucin
SP	Surfactant protein
CC	Clara cell
TTF-1	Thyroid transcription factor 1
ALDH1	Aldehyde dehydrogenase 1
SOX2	Sex determining region Y-box 2
OCT-4	Octamer binding transcription factor 4
OR	Odds ratio
TRU	Terminal respiratory unit

Introduction

Adenocarcinoma of the lung is the most common histological type of primary lung cancer[1] and is a heterogeneous tumor with diverse molecular, clinical, and pathological characteristics. Identification of molecular driver mutations and their therapeutic implications in lung adenocarcinoma have become an important area of research as evidenced by the abundance of genomic, mutational, and proteomic profiling studies.[2, 3] Many studies have shown correlations between morphological features and molecular alterations in lung adenocarcinoma. Previous reports have investigated the association between epidermal growth factor receptor (*EGFR)* mutations and specific histological subtypes of adenocarcinoma such as lepidic (formerly known as nonmucinous bronchioloalveolar carcinoma), papillary, and micropapillary patterns.[4-7] In contrast, *K-ras* mutation status has been shown to be significantly associated with solid and invasive mucinous adenocarcinoma subtypes.[8, 9] Therefore, these findings raise the fundamental question of whether

morphological features reflect the presence of molecular alterations.

The presence of anaplastic lymphoma kinase (*ALK*) gene rearrangement in lung adenocarcinomas is the best predictor of response to crizotinib, an ALK tyrosine kinase inhibitor.[10, 11] Fluorescence *in situ* hybridization (FISH) has been established as the gold standard method for the detection of *ALK* rearrangement in lung adenocarcinoma. The Food and Drug Administration approved crizotinib with a companion diagnostic FISH test for *ALK*-rearranged non-small cell lung cancer (NSCLC). Several studies have investigated the predictive value of pathological and morphological features in detecting *ALK*-rearranged tumors; however, the results of these studies have been inconsistent because of the limited number of *ALK*-rearranged tumors.[12-16] Solid signet-ring cell subtypes and cribriform pattern have been associated with *ALK* rearrangement in lung adenocarcinoma.[12, 15] A few studies have reported a positive histological correlation with *ALK* rearrangement in lung adenocarcinoma using the new International Association for the Study of Lung Cancer, American Thoracic Society and European Respiratory Society

(IASLC/ATS/ERS) classification that was published in 2011.[16, 17] However, the comparative analysis of these histomorphological features and subtypes of *ALK*-rearranged lung adenocarcinoma based on driver oncogene mutations has not been clearly established in lung adenocarcinoma.

In addition, it's widely recognized that rearrangements of *ALK* are more often found in younger age patients with advanced stage at diagnosis.[16] However, the biologic behavior and mechanism of *ALK*-rearranged lung adenocarcinoma has not been elucidated. We hypothesized that epithelial-mesenchymal transition (EMT), that is an important step in the invasion and progression of cancer, may contribute to the characteristic biologic behavior of *ALK*-rearranged lung adenocarcinoma. Cancer cells undergoing EMT can acquire invasive properties and enter the surrounding stroma, resulting in the creation of a favorable microenvironment for cancer progression and metastasis.[18, 19] Furthermore, recent findings demonstrate that the two novel concepts, EMT and cancer stem cell (CSC) theory, have merged in cancer biology.[20] Studies show that EMT cells (e.g., epithelial cells with loss of E-cadherin

expression) acquire stem cell characteristics, that maintenance of the stem cell state depends on continuous EMT-inducing signals, and that signaling pathways involved in stemness also act as potent EMT inducers.[21, 22]

The aim of this study was 1) to evaluate the clinicopathological and histological features of 80 cases of *ALK*-rearranged resected lung adenocarcinomas and compare these features with those of *ALK*-negative tumors expressing well-known driver mutations associated with lung adenocarcinoma, 2) to investigate the correlation between molecular subtype and histological features of lung adenocarcinoma based on the new IASLC/ATS/ERS classification, and 3) to investigate the EMT and CSC marker expressions according to molecular subtypes in lung adenocarcinoma.

Materials and Methods

Case selection

A total of 80 surgically resected lung adenocarcinoma specimens harboring *ALK*-rearrangement were retrieved from the files of Seoul National University Affiliated Hospitals and the Asan Medical Center between January 2004 and June 2011. In addition, 213 *ALK*-negative resected adenocarcinoma specimens obtained from patients diagnosed between March 2009 and March 2010 were included in the study. Of the 213 *ALK*-negative tumors, 91 were *EGFR*-mutated, 29 were *K-ras*-mutated, and 93 were triple-negative (TN; wild-type *EGFR*, *K-ras*, and *ALK*). Patients who had a previous history of cancer, presurgical chemotherapy or radiotherapy were excluded. All cases were classified according to the seventh edition of the Union for International Cancer Control/American Joint Committee on Cancer TNM classification.[23] Clinicopathological information was obtained from the medical records and pathology reports. This study was approved by the Institutional Review

Board at Seoul National University Bundang Hospital.

Histological anaylsis

All resected specimens were fixed with formalin and stained with hematoxylin and eosin (H&E). All slides, including those of normal lung tissue, were carefully reviewed by 2 of the authors (H.K. and J.H.C.). An average of 8.9 slides (range: 1–14 slides) from each case was reviewed. Recent reports have demonstrated a strong association of extracellular mucin and cribriform pattern with *ALK*-rearranged tumors.[24] Therefore, the presence of extracellular mucin and cribriform architecture and the proportion of mucin-containing cells were evaluated in *ALK*-rearranged and *ALK*-negative tumors. *ALK*-rearranged tumors tended to be centrally located near the bronchus; therefore, the anatomic relationship between the tumor and the bronchi was investigated. The following histological parameters were evaluated: tumor location in relation to the bronchus; tumor invasion to the bronchus; alterations in bronchial epithelial cells located adjacent to the tumor; psammomatous

calcifications; cholesterol cleft; tumor size; pathological stage; and visceral pleural, vascular, and lymphatic invasion. Adenocarcinoma *in situ* and minimally invasive adenocarcinoma cases were excluded from the study. All invasive adenocarcinomas were categorized as lepidic, acinar, papillary, solid, micropapillary predominant, and invasive mucinous adenocarcinoma (IMA) according to the IASLC/ATS/ERS classification.[17]

Detection of *ALK* gene rearrangement

FISH was performed on formalin fixed paraffin embedded (FFPE) tumor tissues using a break-apart probe specific to the *ALK* locus (Vysis LSI ALK dual-color, break-apart rearrangement probe; Abbott Molecular, Abbott Park, IL) according to the manufacturer's instructions. FISH-positive cases were defined as those presenting more than 15% split signals or an isolated red signal in tumor cells, as described previously.[20-22] Briefly, 3-㎛-thick sections from FFPE tissue blocks were deparaffinized, dehydrated, immersed in 0.2N HCl, and washed. The sections were

immersed in 0.01M citrate buffer, boiled in a microwave for 5 minutes, treated with pretreatment reagent (Abbott Molecular) at 80℃ for 30 minutes, and reacted with protease mixed with a protease buffer. Dual-probe hybridization was performed using the LSI ALK dual-color probe, which hybridizes to the 2p23 band with SpectrumOrange (red) and SpectrumGreen on either side of the *ALK* gene breakpoint (Abbott Molecular). After applying the probe mixture, they were treated with protease, incubated in a humidified atmosphere with HybriteTM (Abbott Molecular) at 75℃ for 5 minutes to denature the probe and target the DNA, and incubated at 37℃ for 16 hours to allow hybridization. They were then immersed in 0.3% NP-40 (Abbott Molecular)/2x saline sodium citrate for washing. For the nuclei counterstaining, 4,6-diamidino-2-phenylindole II and an antifade compound (p-phenylenediamine) were applied. Signals for each probe were evaluated under a microscope equipped with a triple-pass filter (diamidino-2-phenylindole/Green/Orange; Abbott Molecular) and an oil immersion objective lens. FISH tests were performed without knowledge of the immunohistochemical (IHC)

results for ALK.

Detection of *EGFR* and *K-ras* mutations

Genomic DNA was extracted from FFPE tissues. After deparaffinization with xylene, tissue sections were stained with H&E, and target lesions were selectively dissected to minimize contamination with normal tissue. Genomic DNA was isolated using the QIAamp DNA Mini Kit (Qiagen, Hilden, Germany) according to the manufacturer's instructions. We analyzed *EGFR* mutations at exon 18 to 21 and *K-ras* mutations at codons 12, 13, and 61 by nested polymerase chain reaction (PCR) and direct DNA sequencing method as described previously.[25] PCR amplification was performed in a total volume of 20 μL volume containing 10 mM Tris-HCl (pH 8.3), 50 mM KCl, 1.5 mM MgCl2, 2.5 mM deoxynucleotide triphosphates, 0.5 μM of each primer, and 0.9 units Taq DNA polymerase (Takara Bio, Shiga, Japan). After preincubation at 94℃ for 2 minutes, DNA was amplified for 35 cycles under the following conditions: denaturation at 94℃ for30 seconds and annealing and elongation at 72℃ for 30

seconds. The PCR products were processed with Big Dye Terminator version 3.1 cycle sequencing kit (Applied Biosystems, Foster, CA), and sequence data were generated with the ABI PRISM 3100 DNA Analyzer (Applied Biosystems). These sequences and chromatographs were manually confirmed with the *EGFR* and *K-ras* reference sequences.

Immunohistochemistry

Immunohistochemistry was performed on tissue microarray sections. Four-micrometer-thick sections were transferred to poly-L-lysine-coated glass slides and incubated in a dry oven at 60℃ for 1 h. The sections were then dewaxed in xylene (3 changes), rehydrated in a descending series of graded ethanol concentrations, and rinsed in Tris-buffered saline (TBS; pH 7.4). The endogenous peroxidase activity was blocked using 5% hydrogen peroxide in methanol for 15 min at 37℃. For antigen retrieval, the slides were placed in citrate buffer (10% citrate buffer stock in distilled water, pH 6.0) and microwaved for 10 min. Nonspecific staining was blocked using

1% horse serum in TBS (pH 7.4) for 3 min. The primary antibodies and their applications are listed in Table 1.Immunostaining was developed using an avidin–biotin–peroxidase complex (Universal Elite ABC Kit; PK-6200; Vectastain, Burlingame, CA, USA) and diaminobenzidine tetrahydrochloride solution (HK153-5K; Biogenex, San Ramon, CA, USA). Positive controls (samples with known reactivity for the antibody) and negative controls (omission of the primary antibody) were included in each assay. Mucin (MUC), surfactant protein (SP) and clara cell protein 10 (CC10) immunostaining was scored as the percentage of positively stained neoplastic cells: 0, no positively stained cells; 1+, 0–24% positively stained cells; 2+, 25–49% positively stained cells; 3+, 50–74% positively stained cells; and 4+, 75–100% positively stained cells. Immunostaining present in the cytoplasm, cell apex (luminal surface), and associated secretory products (luminal contents) was evaluated separately. Cells were considered positive when at least 1 of these components stained positively. Cytoplasmic, luminal surface, or luminal immunostaining in ≥25% of tumor cells (score ≥ 2) was considered positive for MUC-1, MUC-2, MUC-5AC,

SP-A, SP-B, SP-C and CC10.[26] For thyroid transcription factor (TTF)-1, p63 and p40 nuclear immunostaining in >10% of tumor cells was considered positive.[14] Immunostaining of EMT markers (E-cadherin and vimentin) and CSC markers (CD133, CD44, aldehyde dehydrogenase 1 (ALDH1), sex determining region Y-box 2 (SOX2), octamer binding transcription factor 4 (OCT4), and nanog) was scored using a semiquantitative approach; the percentage of positive tumor cells (0–100%) was multiplied by the staining intensity (0, negative; 1, weak; 2, moderate; 3, strong) to generate a total score ranging from 0-300 for each sample. Samples with a score of 0–100 and 101–300 were classified as negative and positive, respectively.[27]

Statistical analysis

Pearson's Chi-square test, Fisher's exact test, and one-way analysis of variance were used to evaluate association of clinicopathological and histological variables with lung adenocarcinoma genotype. Multivariate logistic regression analysis was used to determine the most significant morphological features associated with *ALK*-

rearranged tumors. All statistical tests were two-sided, and a p value <0.05 was considered statistically significant. All analyses were performed using SPSS version 18.0 (SPSS Inc., Chicago, IL, USA).

Results

Patient characteristics

The clinicopathological characteristics of the 293 patients are listed in Table 2. Of the 293 patients, 147 (50.2%) were men and 146 (49.8%) were women. The median age was 62.0 years (range, 30 to 83 years). Of the 293 patients, 175 patients (59.7%) were never-smokers and 118 (40.3%) were smokers (68, ex-smokers; 50, current-smokers). Acinar predominant (44.7%) was the most common histological subtype, followed by solid predominant (21.2%), papillary predominant (20.8%), lepidic predominant (5.5%), micropapillary predominant (4.4%), and IMA (3.4%). According to pathological stage, 61.1%, 15.0%, 21.2%, and 2.7% of the cases were p-stage I, stage II, stage III, and stage IV, respectively.

Comparison of the clinicopathological features between *ALK*-rearranged and *ALK*-negative tumors

The clinicopathological features of lung adenocarcinoma according to mutation status are shown in Table 3. *ALK*-rearranged tumors were significantly associated with younger age at presentation, frequent nodal metastasis, and higher stage of disease at diagnosis when compared with *ALK*-negative tumors ($p < 0.001$). The median age of patients with *ALK*-rearranged tumors was 55.8 years, whereas the median age of patients with *EGFR*-mutated, *K-ras*-mutated, and TN tumors was 63.3, 64.9, and 65.1 years, respectively. Of the 80 patients with *ALK*-rearranged tumors, 59.0% (46/80) showed nodal metastasis at diagnosis and 50.0% (40/80) presented with advanced stage (III or IV) disease. The frequency of *ALK*-rearranged (55.0%; 44/80) and *EGFR*-mutated (68.0%; 61/91) tumors was significantly higher ($p < 0.001$) in female patients than that of *K-ras*-mutated (31.0%; 9/29) and TN (34.4%; 32/93) tumors. *ALK*-rearranged (70.0%; 56/80) and *EGFR*-mutated (70.3%; 64/91) tumors were significantly higher ($p < 0.001$) in never-smokers than *K-ras*-mutated (41.4%; 12/29) and TN (46.2%; 43/93) tumors. Tumor size was not significantly different between *ALK*-rearranged and *ALK*-negative tumors.

Histomorphological findings

Comparison of the morphological features between ALK-rearranged and ALK-negative tumors

Focal cribriform formation was present in 40.0% (32/80) of *ALK*-rearranged tumors (Figure 1A). Significant extracellular mucin and mucin-containing cells, including goblet cells (Figure 1B) and signet-ring cells (Figure 1C), were observed in 57.5% (46/80) and 62.5% (50/80) of *ALK*-rearranged tumors, respectively (Table 4). Three *ALK*-rearranged tumor cases showed morphology similar to IMA, including a predominant lepidic pattern of goblet cell proliferation with abundant extracellular mucin. We noted that mucin containing tumor cells resemble the non-neoplastic goblet cells in segmental bronchus or bronchiole level. Several tumor glands resembled adjacent bronchial gland in morphology (Figure 2A). In some *ALK*-rearranged cases, tumor cells invaded the adjacent bronchiolar epithelium and showed the appearance of 'budding off' of small epithelial cell clusters into the lumen (Figure 2B). Furthermore, flat atypical epithelial lesions that resembled adjacent

tumor cells infiltrated the non-neoplastic bronchial epithelium. This close anatomic relationship with the bronchus was observed in 86.3% (69/80) of *ALK*-rearranged tumors. Psammoma bodies (Figure 1D) and cholesterol clefts (Figure 1E) were observed in 56.4% (44/80) and 40.5% (32/80) of *ALK*-rearranged tumors, respectively. All the morphological characteristics described above were less evident in *ALK*-negative tumors ($p < 0.001$).

Correlation between molecular subtype and histological features of lung adenocarcinoma based on the new IASLC/ATS/ERS classification

The histomorphological features of the 4 molecular subtypes based on the new IASLC/ATS/ERS lung adenocarcinoma classification are summarized in Table 4. *ALK*-rearranged tumors showed various histological patterns. The frequency of a solid predominant pattern was significantly higher in *ALK*-rearranged tumors than in *ALK*-negative tumors (43.8%; 35/80; $p < 0.001$). In contrast, the frequency of acinar predominant histology was significantly lower in *ALK*-rearranged tumors than in

ALK-negative tumors (28.7%; 23/80; $p < 0.001$). In contrast to *ALK*-negative tumors, lepidic predominant histology was not observed in *ALK*-rearranged tumors ($p = 0.003$). For *EGFR*-mutated and TN tumors, acinar predominant pattern was the most frequently observed histology (*EGFR*-mutated: 58.2%, 53/91; TN: 40.9%), followed by papillary predominant pattern (*EGFR*-mutated: 24.2%, 22/91; TN: 20.4%, 19/93). Acinar predominant was the most frequently observed pattern in *K-ras*-mutated tumors (58.6%; 17/29), followed by solid predominant (17.2%; 5/29). IMA was rarely observed in *ALK*-rearranged (3.7%; 3/80), *EGFR*-mutated (2.2%; 2/91), and TN (5.4%; 5/93) tumors. Histological patterns are assessed semiquantitatively in 5% increments in the new IASLC/ATS/ERS classification. Therefore, all visible patterns over 5% were recorded, and tumors were classified according to the presence of any histological subtype. The frequency of at least 5% solid pattern was significantly higher in *ALK*-rearranged tumors than in *ALK*-negative tumors (67.5%, 19.8%, 37.9%, and 26.9% of *ALK*-rearranged, *EGFR*-mutated, *K-ras*-mutated, and TN tumors, respectively; $p < 0.001$). Acinar and lepidic patterns were less frequently

observed in *ALK*-rearranged tumors than in *ALK*-negative tumors (acinar, 53.8%; lepidic, 12.5%; $p < 0.001$). The frequency of at least 5% acinar pattern (90.1%) and at least 5% lepidic pattern (57.1%) was significantly higher in *EGFR*-mutated tumors when compared with the other molecular subtypes ($p < 0.001$). *EGFR*-mutated tumors had the lowest frequency of solid pattern among the 4 molecular subtypes (19.8%; $p < 0.001$).

Immunohistochemical findings

Correlation between molecular subtype and immunohistochemical features of lung adenocarcinoma

Several molecular markers were evaluated to investigate the origin of *ALK*-rearranged tumors. Type II pneumocytes served as a positive control for the expression of MUC and SPs. MUC-2, MUC-5Ac and CC10 were not expressed in lung tumors. A high positive rate of MUC-1, SP-A, and SP-B expression was present in all subgroups. The positive rate of MUC-1 and SP immunostaining was not

significantly different between *ALK*-rearranged tumors and *ALK*-negative tumors (Table 5). TTF-1 positivity was more frequently observed in *EGFR*-mutated tumors (100%) than in *ALK*-rearranged (70%), *K-ras*-mutated (69%), and TN (70.8%) tumors ($p = 0.001$). In contrast, p63 immunostaining was significantly higher in *ALK*-rearranged tumors than in *ALK*-negative tumors (67.1%, 4.3%, 14.3%, and 14.6% of *ALK*-rearranged, *EGFR*-mutated, *K-ras*-mutated, and TN tumors, respectively; $p < 0.001$). P40 positivity was observed in low frequency in all subgroups (2.9%, 4.3%, 7.1%, and 4.2% of *ALK*-rearranged, *EGFR*-mutated, *K-ras*-mutated, and TN tumors, respectively; $p > 0.05$).

Expression of epithelial mesenchymal transition markers and cancer stem cell markers according to molecular subtypes

Combined loss of E-cadherin and expression of vimentin, a representative marker of EMT, was more commonly observed in *ALK*-rearranged tumors than other genotypes (38.9%, 19.1%, 26.9% and 14.6% of *ALK*-rearranged, *EGFR*-mutated, *K-ras*-

mutated, and TN tumors, respectively; p =0.015; Table 5; Figure 3). Regarding CSC markers, CD133, CD44 and ALDH1 were strongly expressed in peribronchial mucus glands and scattered throughout the bronchial epithelium, but it was not detected in type II pneumocytes, whereas SOX2, OCT4, and nanog were not expressed in normal lung tissue. Expression of CD133, CD44, ALDH1 and nanog was observed in 58.8%, 23.5%, 41.2% and 62.4% of *ALK*-rearranged subtype, however there was no difference between other genotypes (Table 5).

Multivariate analysis

Results of the multivariate analysis are shown in Table 6. *ALK*-rearranged lung adenocarcinoma was significantly associated with the following morphological characteristics: cribriform formation (odds ratio [OR], 3.253; p = 0.028), presence of mucin-containing cells (OR, 4.899; p = 0.008), close relationship to adjacent bronchioles (OR, 5.361; p = 0.001), and presence of psammoma bodies (OR, 4.026; p = 0.002). *ALK*-rearranged tumors were also significantly associated with solid

predominant histological subtype (OR, 13.685; $p = 0.023$).

Discussion

In this study, we performed a detailed comprehensive analysis of the histomorphological features associated with *ALK*-rearranged lung adenocarcinoma based on comparisons with well-known driver oncogene mutations. We found that *ALK*-rearranged tumors were significantly associated with younger age at presentation, frequent nodal metastasis, and higher stage of disease at diagnosis. Furthermore, *ALK*-rearranged lung adenocarcinoma exhibited several histological characteristics that differentiated it from other genotypes: cribriform formation, presence of mucin-containing cells, close relationship to adjacent bronchioles, presence of psammoma bodies, and solid predominant histological subtype. Correlation of histological characteristics with molecular alterations in lung adenocarcinoma may provide a new approach to refine pathological classification and its clinical relevance. To the best of our knowledge, this is the largest comprehensive analysis comparing the histomorphological features of resected *ALK*-rearranged

tumors with other genotypes.

Histomorphological features specific to *ALK*-rearranged tumors have been reported, including cribriform formation and the presence of mucin or mucin-containing cells and psammoma bodies.[16, 24] We also found that these features were strongly associated with *ALK*-rearranged tumors. We also identified that a close relationship to the adjacent bronchial epithelium is a unique feature of *ALK*-rearranged tumors. This close relationship with the bronchus was observed in 86.3% of *ALK*-rearranged tumors. Mucin containing tumor cells resembling the non-neoplastic goblet cells in segmental bronchus or bronchiole level were observed, and several tumor glands resembled the adjacent bronchial gland in morphology. In a few *ALK*-rearranged cases, tumor cells invaded the adjacent bronchiolar epithelium and showed the appearance of "budding off" of small epithelial cell clusters into the lumen. Furthermore, flat atypical lesions that resembled adjacent tumor cells infiltrated the non-neoplastic bronchial epithelium. *ALK*-rearranged tumors were more likely to be centrally located and easily obtained from the bronchoscopic biopsy procedure.

Based on these results, we hypothesized that *ALK*-rearranged tumors, in contrast to EGFR-mutated tumors, may represent non-TRU-type adenocarcinoma and therefore originate from bronchial epithelial cells. Histologically, the series of cells ranges from nonciliated, small bronchioles to pneumocytes, which we named the "TRU" and the master molecule TTF-1 is expressed in a subset of lung adenocarcinomas characterized by morphological similarity to the cells comprising the TRU, such as type II pneumocytes, Clara cells, and nonciliated bronchioles. Thus, this subset of adenocarcinomas comprises a clade that is related to the TRU type adenocarcinoma. In contrast, non-TRU type adenocarcinoma was related with bronchus-associated cells such as bronchial surface epithelium and glandular cells as a normal counterpart and low TTF-1 expression. To elucidate this hypothesis, we performed immunostaining for markers of mucus cell (MUC), basal cell (p63 and p40), clara cell (CC10), and type II pneumocyte (SP and TTF-1). However, the expression of MUC-1, SP-A, SP-B, and SP-C was not different between *ALK*-rearranged and *ALK*-negative tumors. In contrast, TTF-1 and p63 expression was significantly different

between *ALK*-rearranged and *ALK*-negative tumors, especially *EGFR*-mutated tumors. TTF-1 positivity was lower in *ALK*-rearranged tumors than in *EGFR*-mutated tumors, whereas p63 positivity was higher in *ALK*-rearranged tumors than in *EGFR*-mutated tumors. Although the frequency of TTF-1 positivity in *ALK*-rearranged tumors suggested they were of TRU-type origin, type II pneumocytes and Clara cells, which are characteristic of TRU-type, are typically negative for p63.[14] Our results suggested that a different mechanism mediates the development of *ALK*-rearranged tumors. We also evaluated the expression of p40 (△Np63) protein by immunohistochemistry. In contrast to p63, p40 positivity was less frequently observed in *ALK*-rearranged tumors (2.9%). p63 and p40 have been shown to be overexpressed especially in squamous cell carcinoma of lung and regarded as a marker of squamous differentiation.[28-32] However, several studies reported that p63 expression was seen in variable frequency (up to 30%) and extent (10 to 70% of tumor cells) in lung adenocarcinoma, whereas p40 was rarely expressed in adenocarcinoma.[33] In addition, Sakai et al. reported 7 out of 9 *ALK*-rearranged

tumors expressed p63, but none of *ALK*-rearranged tumors expressed p40.[34] Our results are similar to those of these studies. We suggested that overexpression of p63 might have functional roles related with carcinogenesis or tumor differentiation rather than squamous markers in lung adenocarcinomas, but further investigation of the significance of p63 expression in lung adenocarcinoma is warranted. In the diagnostic point of view, spatial proximity between bronchus and *ALK*-rearranged tumors and frequent solid histologic subtype with p63 expression may cause diagnostic difficulties to differentiate squamous cell carcinoma in the small biopsy, whereas p40 was rarely expressed in *ALK*-rearranged adenocarcinoma. Awareness of these features may help pathologists diagnose accurately.

Our results revealed that the predominant histological subtype varied according to the status of driver mutations in *ALK*, *EGFR*, and *K-ras*. In contrast to *ALK*-negative tumors, *ALK*-rearranged tumors were significantly associated with solid predominant subtype and not acinar or papillary predominant subtypes. *ALK*-rearranged tumors exhibited aggressive behavior such as nodal metastasis, advanced disease stage at

diagnosis, and lymphovascular invasion. In contrast, *EGFR*-mutated tumors were significantly associated with acinar or papillary predominant subtypes. Although the lepidic predominant subtype was not significantly correlated with *EGFR* mutation, a significant correlation between lepidic component presence and *EGFR* mutation was observed. *EGFR*-mutated tumors have been shown to exhibit nonaggressive behavior, such as decreased nodal metastasis and lymphovascular invasion. In the present study, the frequency of acinar and solid predominant patterns was higher in *K-ras*-mutated tumors than micropapillary and lepidic predominant patterns; however, it is difficult to assess the pathological relevance of these findings because of the small number of *K-ras*-mutated tumors. TN tumors were associated with acinar, papillary, and solid predominant patterns.

We suggested that EMT may be related with aggressive biologic behavior of *ALK*-rearranged tumors. EMT is a dedifferentiation program that converts epithelial cells into a mesenchymal phenotype and is involved in embryogenesis and used pathologically during cancer progression.[18] Loss of functional expression of E-

cadherin and expression of mesenchymal markers such as vimentin and N-cadherin is presently considered as the hall mark of EMT. Thus, we performed immunostaining for E-cadherin and vimentin, as a representative marker of EMT phenotype and observed that loss of E-cadherin and expression of vimentin were frequently observed in *ALK*-rearranged tumors. EMT phenotype is the characteristic finding of *ALK*-rearranged tumors compared with other genotypes, and this could potentially be a contributing feature to the frequent metastases and high tumor stage seen in *ALK*-rearranged tumors.

Next, we investigated the CSC properties of *ALK*-rearranged tumor. Recent studies have shown evidence suggesting that the two novel concepts, EMT and CSCs, have merged in cancer biology.[20] The studies have consistently demonstrated that EMT cells acquire stem cell characteristics in breast, ovary, pancreas and prostate cancers.[35-38] Additional recent studies suggest that some important signaling pathways involved in stemness also act as potent EMT inducers in different cellular or biological contexts.[39, 40] Thus, we suggested that CSC phenotype may be

associated with ALK-rearranged tumors, like EMT phenotype. We evaluated several markers such as CD133, CD44, ALDH1, SOX2, OCT-4 and nanog that have been proposed as putative CSC markers in NSCLC.[41] However, there was no correlation between CSC marker expression and molecular subtypes in lung adenocarcinoma. Further study is needed to elucidate the biological role and relationship with EMT of CSC markers in lung adenocarcinoma.

In conclusion, *ALK*-rearranged lung adenocarcinoma exhibited distinct clinicopathological and morphological features compared with other genotypes. Knowledge of these features may improve the diagnostic accuracy and lead to a better understanding of the characteristic behavior of *ALK*-rearranged tumors.

References

1. Devesa SS, Bray F, Vizcaino AP, Parkin DM. International lung cancer trends by histologic type: male:female differences diminishing and adenocarcinoma rates rising. Int J Cancer 2005; 117: 294-299.

2. Weir BA, Woo MS, Getz G et al. Characterizing the cancer genome in lung adenocarcinoma. Nature 2007; 450: 893-898.

3. Ding L, Getz G, Wheeler DA et al. Somatic mutations affect key pathways in lung adenocarcinoma. Nature 2008; 455: 1069-1075.

4. Hsieh RK, Lim KH, Kuo HT et al. Female sex and bronchioloalveolar pathologic subtype predict EGFR mutations in non-small cell lung cancer. Chest 2005; 128: 317-321.

5. Motoi N, Szoke J, Riely GJ et al. Lung adenocarcinoma: modification of the 2004 WHO mixed subtype to include the major histologic subtype suggests correlations between papillary and micropapillary adenocarcinoma subtypes, EGFR

mutations and gene expression analysis. Am J Surg Pathol 2008; 32: 810-827.

6. Ninomiya H, Hiramatsu M, Inamura K et al. Correlation between morphology and EGFR mutations in lung adenocarcinomas Significance of the micropapillary pattern and the hobnail cell type. Lung Cancer 2009; 63: 235-240.

7. Sun PL, Seol H, Lee HJ et al. High incidence of EGFR mutations in Korean men smokers with no intratumoral heterogeneity of lung adenocarcinomas: correlation with histologic subtypes, EGFR/TTF-1 expressions, and clinical features. J Thorac Oncol 2012; 7: 323-330.

8. Rekhtman N, Ang DC, Riely GJ et al. KRAS mutations are associated with solid growth pattern and tumor-infiltrating leukocytes in lung adenocarcinoma. Mod Pathol 2013.

9. Finberg KE, Sequist LV, Joshi VA et al. Mucinous differentiation correlates with absence of EGFR mutation and presence of KRAS mutation in lung adenocarcinomas with bronchioloalveolar features. J Mol Diagn 2007; 9: 320-326.

10. Kwak EL, Bang YJ, Camidge DR et al. Anaplastic lymphoma kinase

inhibition in non-small-cell lung cancer. N Engl J Med 2010; 363: 1693-1703.

11. Shaw AT, Yeap BY, Solomon BJ et al. Effect of crizotinib on overall survival in patients with advanced non-small-cell lung cancer harbouring ALK gene rearrangement: a retrospective analysis. Lancet Oncol 2011; 12: 1004-1012.

12. Rodig SJ, Mino-Kenudson M, Dacic S et al. Unique clinicopathologic features characterize ALK-rearranged lung adenocarcinoma in the western population. Clin Cancer Res 2009; 15: 5216-5223.

13. Inamura K, Takeuchi K, Togashi Y et al. EML4-ALK lung cancers are characterized by rare other mutations, a TTF-1 cell lineage, an acinar histology, and young onset. Mod Pathol 2009; 22: 508-515.

14. Yoshida A, Tsuta K, Watanabe S et al. Frequent ALK rearrangement and TTF-1/p63 co-expression in lung adenocarcinoma with signet-ring cell component. Lung Cancer 2011; 72: 309-315.

15. Popat S, Gonzalez D, Min T et al. ALK translocation is associated with ALK immunoreactivity and extensive signet-ring morphology in primary lung

adenocarcinoma. Lung Cancer 2012; 75: 300-305.

16. Nishino M, Klepeis VE, Yeap BY et al. Histologic and cytomorphologic features of ALK-rearranged lung adenocarcinomas. Mod Pathol 2012; 25: 1462-1472.

17. Travis WD, Brambilla E, Noguchi M et al. International association for the study of lung cancer/american thoracic society/european respiratory society international multidisciplinary classification of lung adenocarcinoma. J Thorac Oncol 2011; 6: 244-285.

18. Iwatsuki M, Mimori K, Yokobori T et al. Epithelial-mesenchymal transition in cancer development and its clinical significance. Cancer Sci 2010; 101: 293-299.

19. Thiery JP, Acloque H, Huang RY, Nieto MA. Epithelial-mesenchymal transitions in development and disease. Cell 2009; 139: 871-890.

20. Mani SA, Guo W, Liao MJ et al. The epithelial-mesenchymal transition generates cells with properties of stem cells. Cell 2008; 133: 704-715.

21. Liu J, Brown RE. Immunohistochemical detection of epithelialmesenchymal transition associated with stemness phenotype in anaplastic

thyroid carcinoma. Int J Clin Exp Pathol 2010; 3: 755-762.

22. Bao B, Azmi AS, Ali S et al. The biological kinship of hypoxia with CSC and EMT and their relationship with deregulated expression of miRNAs and tumor aggressiveness. Biochim Biophys Acta 2012; 1826: 272-296.

23. Sobin LH GM WC. TNM Classification of Malignant Tumours Seventh edition. . 2009.

24. Yoshida A, Tsuta K, Nakamura H et al. Comprehensive histologic analysis of ALK-rearranged lung carcinomas. Am J Surg Pathol 2011; 35: 1226-1234.

25. Chung JH, Choe G, Jheon S et al. Epidermal growth factor receptor mutation and pathologic-radiologic correlation between multiple lung nodules with ground-glass opacity differentiates multicentric origin from intrapulmonary spread. J Thorac Oncol 2009; 4: 1490-1495.

26. Tsutsumida H, Goto M, Kitajima S et al. Combined status of MUC1 mucin and surfactant apoprotein A expression can predict the outcome of patients with small-size lung adenocarcinoma. Histopathology 2004; 44: 147-155.

27. Kim H, Yoo SB, Sun P et al. Alteration of the E-Cadherin/beta-Catenin Complex Is an Independent Poor Prognostic Factor in Lung Adenocarcinoma. Korean J Pathol 2013; 47: 44-51.

28. Bishop JA, Teruya-Feldstein J, Westra WH et al. p40 (DeltaNp63) is superior to p63 for the diagnosis of pulmonary squamous cell carcinoma. Mod Pathol 2012; 25: 405-415.

29. Rekhtman N, Ang DC, Sima CS et al. Immunohistochemical algorithm for differentiation of lung adenocarcinoma and squamous cell carcinoma based on large series of whole-tissue sections with validation in small specimens. Mod Pathol 2011; 24: 1348-1359.

30. Bilal H, Handra-Luca A, Bertrand JC, Fouret PJ. P63 is expressed in basal and myoepithelial cells of human normal and tumor salivary gland tissues. J Histochem Cytochem 2003; 51: 133-139.

31. Wang BY, Gil J, Kaufman D et al. P63 in pulmonary epithelium, pulmonary squamous neoplasms, and other pulmonary tumors. Hum Pathol 2002; 33: 921-926.

32. Pelosi G, Pasini F, Olsen Stenholm C et al. p63 immunoreactivity in lung cancer: yet another player in the development of squamous cell carcinomas? J Pathol 2002; 198: 100-109.

33. Nonaka D. A study of DeltaNp63 expression in lung non-small cell carcinomas. Am J Surg Pathol 2012; 36: 895-899.

34. Sakai Y, Nakai T, Ohbayashi C et al. Immunohistochemical Profiling of ALK Fusion Gene-Positive Adenocarcinomas of the Lung. Int J Surg Pathol 2013.

35. Santisteban M, Reiman JM, Asiedu MK et al. Immune-induced epithelial to mesenchymal transition in vivo generates breast cancer stem cells. Cancer Res 2009; 69: 2887-2895.

36. Ahmed N, Abubaker K, Findlay J, Quinn M. Epithelial mesenchymal transition and cancer stem cell-like phenotypes facilitate chemoresistance in recurrent ovarian cancer. Curr Cancer Drug Targets 2010; 10: 268-278.

37. Du Z, Qin R, Wei C et al. Pancreatic cancer cells resistant to chemoradiotherapy rich in "stem-cell-like" tumor cells. Dig Dis Sci 2011; 56: 741-

750.

38. Giannoni E, Bianchini F, Masieri L et al. Reciprocal activation of prostate cancer cells and cancer-associated fibroblasts stimulates epithelial-mesenchymal transition and cancer stemness. Cancer Res 2010; 70: 6945-6956.

39. Fuxe J, Vincent T, Garcia de Herreros A. Transcriptional crosstalk between TGF-beta and stem cell pathways in tumor cell invasion: role of EMT promoting Smad complexes. Cell Cycle 2010; 9: 2363-2374.

40. Wellner U, Schubert J, Burk UC et al. The EMT-activator ZEB1 promotes tumorigenicity by repressing stemness-inhibiting microRNAs. Nat Cell Biol 2009; 11: 1487-1495.

41. Sterlacci W, Savic S, Fiegl M et al. Putative stem cell markers in non-small-cell lung cancer: a clinicopathologic characterization. J Thorac Oncol 2014; 9: 41-49.

Table 1. Primary antibodies and conditions

ANTIBODY	CLONE	SOURCE	DILUTION
MUC-1	Ma695	Novocastra	1:100
MUC-2	Ccp58	Novocastra	1:100
MUC-5AC	CLH2	Novocastra	1:100
CC10	FL96	Santa Cruz Biotechnology	1:100
SP-A	PE10	Dako	1:200
SP-B	SPB01	Neomarker	1:100
SP-C	FL-197	Santa Cruz Biotechnology	1:100
TTF-1	8G7G3/1	Dako	1:100
p63	4A4	Zeta Corporation	1:100
p40	rabbitpoly	Biocare	1:200
E-cadherin	SPM471	Thermo Fisher Scientific	1:150
Vimentin	V9	Dako	1:100
CD133	NA	Spring Bioscience	1:200
CD44	156-3C11	Neomarkers	1:200
ALDH1	44	BD Biosciences	1:100
SOX2	D6D9	Cell Signalling	1:100
OCT4	MRQ-10	Cell Marque	1:100
Nanog	EPR2027	Abcam	1:100

Abbreviations: MUC, mucin; CC10, Clara cell 10; SP, surfactant protein; TTF, thyroid transcription factor; ALDH1, aldehyde dehydrogenase 1; SOX2, sex-determining region Y-box 2; OCT4, Octamer-4

Table 2. Clinicopathological characteristics of 293 patients with lung adenocarcinoma.

Characteristics		Patients No. (%)
Sex	Male	147 (50.2)
	Female	146 (49.8)
Age (years)	Median (Range)	62.0 (30-83)
Smoking history	Never	175 (59.7)
	Ex-smoker	68 (23.2)
	Current smoker	50 (17.1)
Tumor size(cm)	Mean (Range)	3.1 (0.7-13.5)
Nodal metastasis		96 (32.8)
Histologic subtype	Lepidic predominant	16 (5.5)
	Acinar predominant	131 (44.7)
	Papillary predominant	61 (20.8)
	Solid predominant	62 (21.2)
	Micropapillary predominant	13 (4.4)
	Invasive mucinous	10 (3.4)
TNM stage	I	179 (61.1)
	II	44 (15.0)
	III	62 (21.2%)
	IV	8 (2.7%)
Total		293 (100%)

Table 3. Clinicopathological characteristics of patients based on driver mutation status

	***ALK* +(n=80)**	***EGFR*+(n=91)**	***K-ras*+(n=29)**	**TN(n=93)**	***p* value**
Sex					***p*<0.001**
M	36(45.0%)	30(33.0%)	20(69.0%)	61(65.6%)	
F	44(55.0%)	61(68.0%)	9(31.0%)	32(34.4%)	
Age (years)					***p*<0.001**
median	55.8	63.3	64.9	65.1	
Smoking history					***p*<0.001**
never	56(70.0%)	64(70.3%)	12(41.4%)	43(46.2%)	
ex-smoker	10(12.5%)	16(17.6%)	10(34.5%)	32(34.4%)	
current smoker	14(17.5%)	11(12.1%)	7(24.1%)	18(19.4%)	
Tumor size(cm)	3.2 ± 1.8	2.7 ± 1.8	3.5 ± 2.7	3.1 ± 1.7	*p*>0.5
Nodal metastasis	46(59.0%)	19(20.9%)	6(24.0%)	25(26.9%)	***p*<0.001**
TNM stage					***p*<0.001**
I	29(36.2%)	71(78.0%)	18(62.1%)	61(65.6%)	
II	11(13.8%)	11(12.1%)	9(31.0%)	13(14.0%)	
III	32(40.0%)	9(9.9%)	2(6.9%)	19(20.4%)	
IV	8(10.0%)	0	0	0	

Abbreviations: TN, triple negative; M, male; F, female

Table 4. Histomorphological characteristics of lung adenocarcinoma based on driver mutation status.

	ALK +(n=80)	*EGFR*+(n=91)	*K-ras*+(n=29)	TN(n=93)	*p* value
Histologic features					
Cribriform formation	32(40.0%)	6(6.6%)	1(3.4%)	18(19.3%)	***p*<0.001**
Extracellular mucin	46(57.5%)	16(17.6%)	5(17.2%)	26(27.9%)	***p*<0.001**
Mucin-containing cells	50(62.5%)	18(19.8%)	5(17.2%)	27(29.0%)	***p*<0.001**
Relation with bronchus	69(86.3%)	39(42.8%)	12(41.4%)	44(47.3%)	***p*<0.001**
bronchiole	52(65.0%)	34(37.4%)	11(37.9%)	31(33.3%)	
segmental bronchus	11(13.8%)	4(4.4%)	0	11(11.8%)	
lobar bronchus	6(7.5%)	1(1.0%)	1(3.4%)	2(2.2%)	
Psammoma body	44(56.4%)	10(11.0%)	1(3.4%)	11(11.8%)	***p*<0.001**
Cholesterol cleft	32(40.5%)	12(13.2%)	2(6.9%)	8(8.6%)	***p*<0.001**
Pleural invasion	36(45%)	31(34.1%)	11(27.9%)	34(36.5%)	*p*>0.05
Vascular invasion	35(43.8%)	21(23.1%)	8(27.6%)	32(34.4%)	***p*=0.033**
Lymphatic invasion	49(62.0%)	31(40.4%)	11(37.9%)	42(45.2%)	***p*=0.047**
Histologic subtypes					
Predominant subtype					
lepidic	0	6(6.6%)	4(13.8%)	6(6.4%)	***p*=0.003**
acinar	23(28.7%)	53(58.2%)	17(58.6%)	38(40.9%)	***p*<0.001**
papillary	17(21.3%)	22(24.2%)	3(10.3%)	19(20.4%)	*p*>0.05
solid	35(43.8%)	5(5.5%)	5(17.2%)	17(18.3%)	***p*<0.001**
micropapillary	2(2.5%)	3(3.3%)	0	8(8.6%)	*p*>0.05
invasive mucinous	3(3.7%)	2(2.2%)	0	5(5.4%)	*p*>0.05
5% of subtype present					
lepidic	10(12.5%)	52(57.1%)	13(44.8%)	28(30.1%)	***p*<0.001**
acinar	42(53.8%)	82(90.1%)	24(82.8%)	69(74.2%)	***p*<0.001**
papillary	31(38.8%)	46(50.5%)	10(34.5%)	42(45.2%)	*p*>0.05
solid	54(67.5%)	18(19.8%)	11(37.9%)	25(26.9%)	***p*<0.001**

micropapillary	12(15.0%)	13(14.3%)	8(27.6%)	21(22.6%)	$p>0.05$
invasive mucinous	3(2.5%)	2(2.2%)	2(6.9%)	7(7.5%)	$p>0.05$

Abbreviations: TN: triple negative

Table 5. Immunohistochemical results for based on driver mutation status.

	ALK +(n=80)	*EGFR*+(n=91)	*K-ras*+(n=29)	TN(n=93)	*p* value
MUC-1 +	98.7%	97.9%	96.3%	95.8%	*p* >0.05
SP-A +	73.7%	63.8%	59.3%	61.4%	*p* >0.05
SP-B +	61.5%	60.5%	59.3%	61.4%	*p* >0.05
SP-C +	25.3%	42.6%	28.6%	39.6%	*p* >0.05
TTF-1 +	70.0%	100%	69.0%	70.8%	***p*=0.001**
p63 +	67.1%	4.3%	14.3%	14.6%	***p*<0.001**
p40	2.9%	4.3%	7.1%	4.2%	*p* >0.05
E-cadherin -	71.3%	29.8%	55.2%	47.9%	***p*<0.001**
Vimentin +	49.3%	31.9%	37.0%	27.1%	*p*=0.063
EMT phenotype*	38.9%	19.1%	26.9%	14.6%	***p*=0.015**
CD133	58.8 %	45.7 %	63.6 %	52.1 %	*p* >0.05
CD44	23.5 %	31.4 %	36.4 %	30.4 %	*p* >0.05
ALDH1	41.2 %	48.6 %	45.5 %	41.1 %	*p* >0.05
Nanog	62.4 %	44.8 %	45.5%	39.60%	*p* >0.05

*: loss of E-cadherin and expression of vimentin

Abbreviations: TN, triple negative; SP, surfactant protein; TTF-1, Thyroid transcription factor 1; ALDH1, aldehyde dehydrogenase 1

Table 6. Multivariate analysis: Factors significantly associated with *ALK* rearrangement on logistic regression analysis.

	Odds ratio	*p* value	95% CI
Cribriform formation	3.253	**0.028**	1.133-9.341
Presence of extracellular mucin	0.775	0.689	0.223-2.691
Presence of mucin-containing cells	4.899	**0.008**	1.521-15.779
Close relation to adjacent bronchioles	5.361	**0.001**	2.032-14.149
Presence of psammoma body	4.026	**0.002**	1.633-9.930
Presence of cholesterol cleft	2.09	0.146	0.773-5.649
Solid predominant pattern	13.685	**0.023**	1.431-130.853

Abbreviations: CI, confidence interval

Figure 1. Histological characteristics of *ALK*-rearranged tumors. A, cribriform formation; B, mucin-containing goblet cells; C, mucin-containing signet-ring cell; D, psammoma body; E, cholesterol cleft.

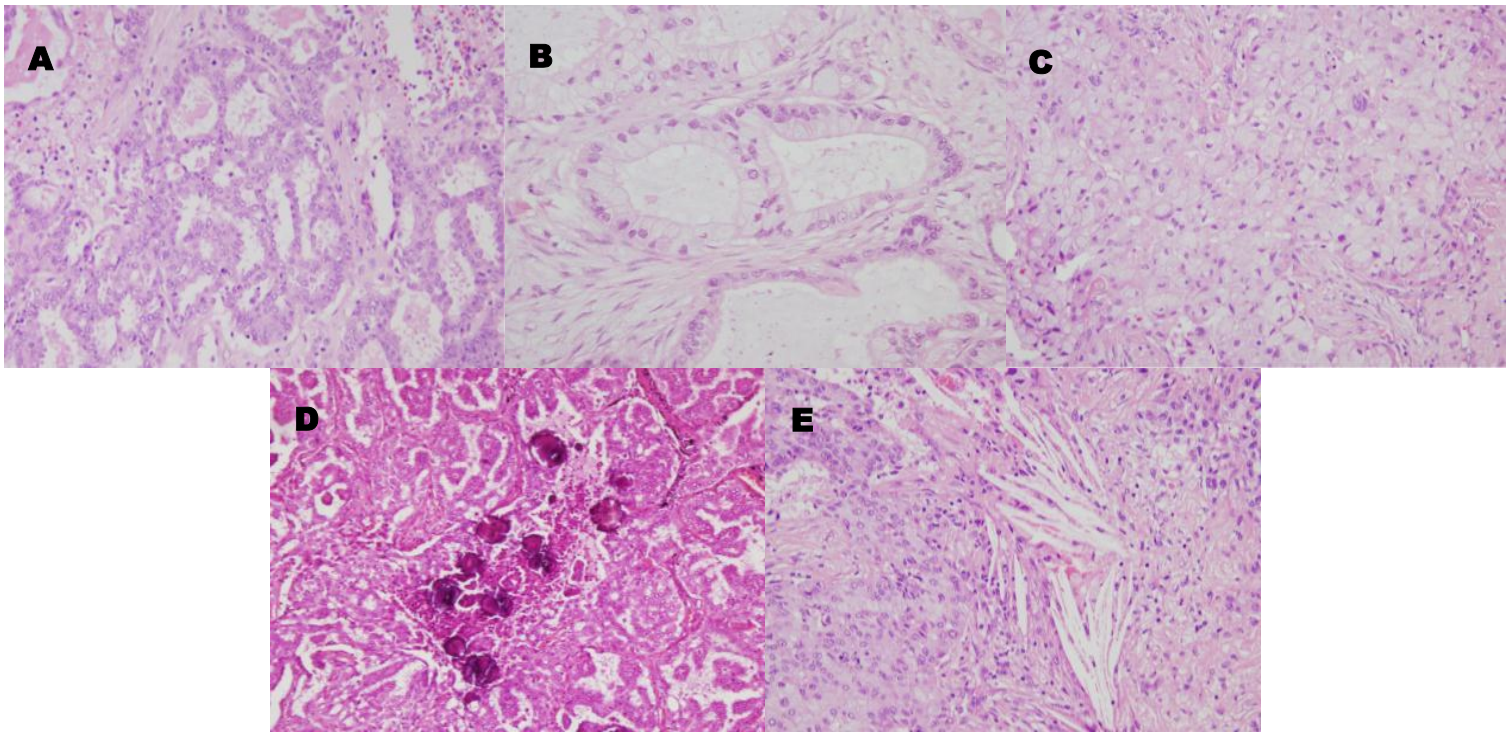

Figure 2. Relationship of *ALK*-rearranged tumors with the bronchiole. A, Tumor gland that resembles the adjacent segmental bronchial gland in morphology; B, Tumor cell infiltration of the adjacent bronchiolar epithelium.

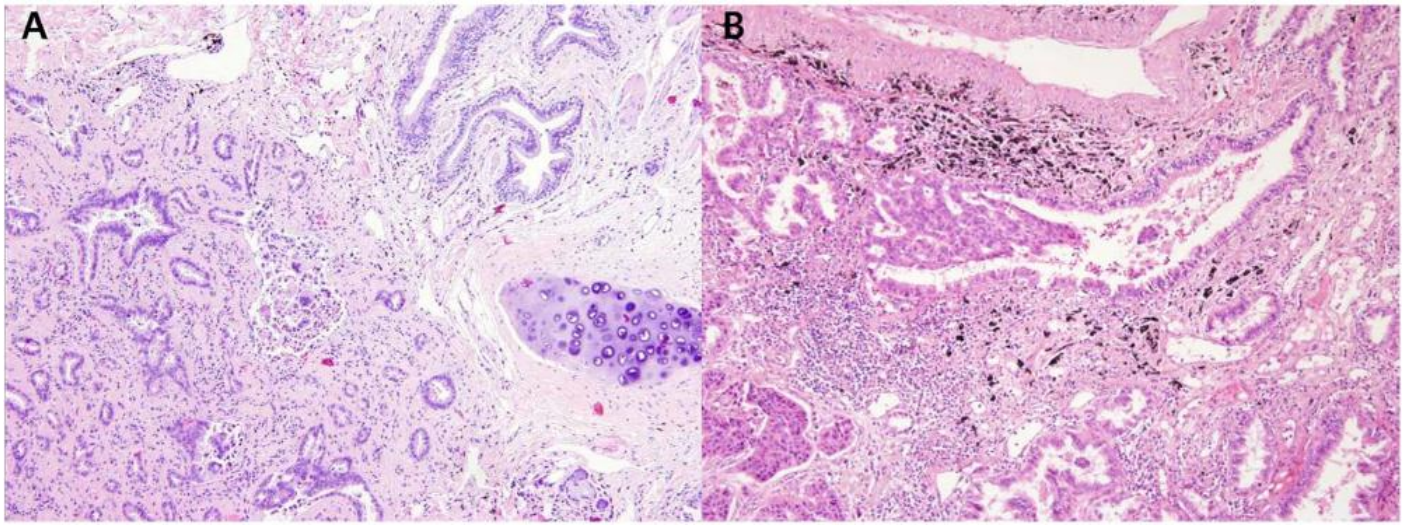

Figure 3. Expression of epithelial mesenchymal transition markers in *ALK*-rearranged tumors. A, Loss of E-cadherin; B, Expression of vimentin.

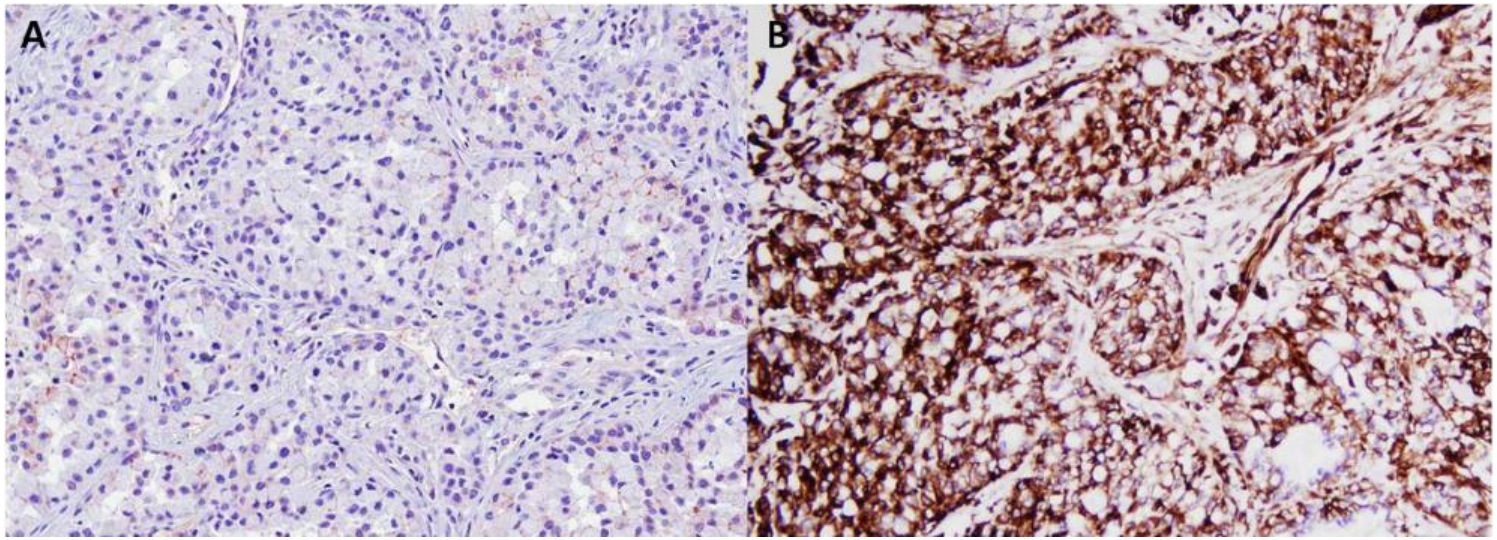

국문초록

배경 및 목적: 폐선암은 조직학적 및 분자유전학적 이질성을 보이는 비소세포폐암의 아형으로 알려져 있으며, 폐선암의 분자유전학적 분류는 조직학적 특징과 연관성이 있다고 보고되고 있다. 본 연구에서는 역형성 림프종 키나아제 (*Anaplastic lymphoma kinase; ALK*) 유전자 전위를 보이는 폐선암의 조직학적 특성과 병태생리학적 기전을 다른 유전자 변이 그룹과 비교 분석하여 그 특성을 규명하고자 하였다.

연구대상 및 방법: 80 례의 *ALK* 유전자 전위 폐선암 조직과 91 례의 상피세포성장인자 수용체 (*epidermal growth factor receptor; EGFR*) 유전자 변이 조직, 29 례의 *K-ras* 유전자 변이 조직 및 93 례의 유전자 변이가 없는 조직을 대상으로 조직학적 특성을 분석하고 면역조직화학염색을 시행하였다.

결과: *ALK* 전위 폐선암은 *ALK* 전위가 없는 폐선암에 비해 높은 비율의 고형성 성장패턴을 보였으며, 다변량 분석에서 *ALK* 전위 폐선암의 특징적인 조직학적 특징으로는 사상형 (cribriform) 패턴의 형성, 점액질을 포함하는 세포의 존재, 주변 세기관지로의 침윤 및 사종체 (psammoma body) 의 존재 등이 확인되었다. *ALK* 전위 폐선암은 임상적 및 조직학적으로 침습적인 성향을 보였으며, 면역조직화학 염색 결과 상피중간엽세

포이행 (Epithelial-mesenchymal transition; EMT) 의 주요 마커인 E-cadherin 의 소실과 vimentin 의 발현을 보였다. 또한 *ALK* 전위 폐선암은 기관지와의 밀접한 연관성을 보이면서 기저세포의 마커로 알려짐 p63의 발현이 빈번하게 관찰되어, 생검조직에서 분화가 나쁜 편평상피암과의 감별이 중요하다는 임상적 의의를 확인하였다.

결론: *ALK* 전위 폐선암은 다른 유전자형을 가진 폐선암과 구별되는 임상병리학적 및 조직학적 소견을 보였다. 이러한 특징을 이해하는 것은 비소세포폐암에 대한 진단의 정확성 향상 및 *ALK* 전위 폐선암의 병태생리학적 특징을 이해하는 데에 도움이 될 수 있다.

주요어 : 폐 신생물, 샘 암종, 폐역형성 림프종 키나아제, 조직학, 유전자형

학번: 2012-30544